Supplementary Information

The eutectic point in choline chloride and ethylene glycol mixtures

Hannah J. Hayler and Susan Perkin*

Physical and Theoretical Chemistry Laboratory, University of Oxford, South Parks Road, Oxford, OX1 3QZ. E-mail: susan.perkin@chem.ox.ac.uk

Differential Scanning Calorimetry

Differential scanning calorimetry (DSC) is a thermal analysis technique that measures the difference in heat flow between sample and reference pans as a function of time and temperature. The reference and sample pans are placed on their respective platforms within the furnace, as per Figure S1(a). Typically, the temperature of the furnace is linearly increased or decreased with time. During the temperature ramp, the sample and reference pan temperatures are kept identical. As the reference and sample pans are identical, if the heat capacity of the sample changes during the ramp, the heat flow to/from the reference pan will need to compensate for the changes to keep the temperatures matched.[1] Therefore, the difference in heat flow between the sample and reference pans will indicate if any thermal transitions have occurred in the sample.

The resulting change in heat flow can be plotted as a function of temperature (a thermogram, see Figure S1(b)) to determine the nature of the transition. Thermal transitions will appear as features on the thermogram *e.g.* steps, peaks or troughs. They can be attributed to chemical or physical changes in the sample and are either endothermic (heat absorbed by the sample) or exothermic (heat released by the sample). Endothermic transitions include melting, glass transitions and evaporation, exothermic transitions include crystallisation, curing and oxidation.

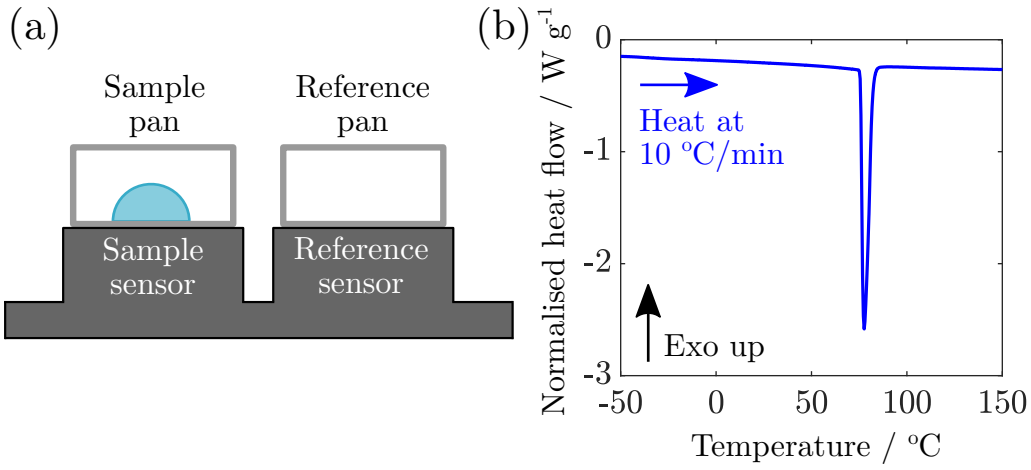

Figure S1 (a) Schematic of the sample and reference platforms in the DSC furnace. (b) Exemplar normalised heat flow as a function of temperature plot (thermogram) when heating the sample at 10 °C/min, showing an endothermic transition.

Crystallisation and melting are of particular interest in this work, and the temperature at which these two transitions occur are determined in different ways. Figure S2(a) shows an exemplar melting transition on heating the sample. The melt begins at the onset temperature (orange open circle) and is complete at the peak of the transition (pink open circle). As the onset temperature defines the point at which the material begins to melt, this is taken as the melting point. To determine the onset temperature, the baseline of the

thermogram is extrapolated (orange dashed line) and the inflectional tangent of the melting peak taken (orange solid line). The point at which these two lines intersect is taken as the onset temperature.

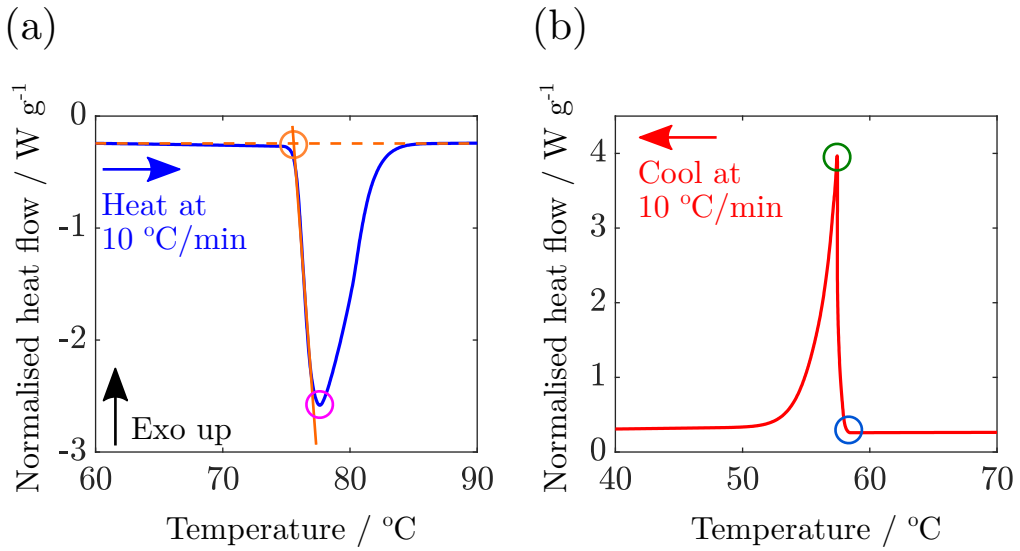

Figure S2 Exemplar normalised heat flow as a function of temperature plots (thermograms) when (a) heating and (b) cooling the sample at 10 ^{o}C/min. The exothermic direction is the same in both plots. (a) An endothermic melting transition. The onset temperature (orange open circle) occurs at the point at which inflectional tangent of the melting peak (orange solid line) intersects the extrapolated baseline (orange dashed line). The peak temperature corresponds to the fully melted material (pink open circle). (b) An exothermic crystallisation transition. The nucleation temperature occurs at the blue open circle, at which point crystal growth begins and is completed at the peak (green open circle).

Figure S2(b) shows an exemplar crystallisation on cooling the sample. As crystallisation is a two-step process involving nucleation and subsequent crystal growth, there are two noticeable features on the thermogram. The open blue circle highlights the temperature at which nucleation occurs. Crystallisation then begins and is complete at the peak temperature highlighted by the open green circle. As the peak temperature defines the point at which the material has fully crystallised, this is taken as the crystallisation point.

Sample Preparation

Individual Components

Ethylene glycol (Sigma-Aldrich, anhydrous, 99.8%) and choline chloride (Sigma-Aldrich, $\geq 99\%$) were used as received.

Deep Eutectic Solvents

Deep eutectic solvents (DESs) were prepared at room temperature and pressure. Ethylene glycol (Sigma-Aldrich, anhydrous, 99.8%) and choline chloride (Sigma-Aldrich, $\geq 99\%$) were used as received.

Choline chloride (ChCl) and ethylene glycol (EG) mixtures were prepared with ChCl mole fractions, $x_{\mathrm{ChCl}} = 0$, 0.001, 0.01, 0.02, 0.03, 0.04, 0.05, 0.06, 0.07, 0.08, 0.09, 0.17, 0.20, 0.25, 0.34, 0.37, 0.50, 0.58, 0.79, 1. The resulting mixture was stirred overnight at 60 ^{o}C and subsequently stored at room temperature and pressure until required.

Once the desired sample had been prepared, the pan and lid type were chosen. All samples used a Tzero aluminium pan with a Tzero lid, for solid samples, or Tzero Hermetic lid, for liquid samples (TA

Intruments). Between 1 and 20 mg of sample was placed in the pan. A pin hole was made in the lid (to allow volatiles to escape and maintain constant pressure), placed on the pan and crimped using the Tzero press (TA Instruments). An identical pan and lid were used to produce a reference in the absence of sample.

Experimental Setup

The reference and sample pans were placed in the cell of the DSC250 (TA Instruments), which was purged under nitrogen at a rate of 50 mL/min. By coupling the DSC to the RCS90 cooling accessory (TA Instruments) the cell could be cooled below room temperature to -90 ^{o}C and heated to a maximum of 550 ^{o}C.

Using the TRIOS software (TA Instruments), the experimental method was designed and subsequently run using the desktop interface. The full method comprised individual segments that controlled the furnace temperature.

Kinetic considerations

Thermodynamically, the freezing point (liquid to solid) and the melting point (solid to liquid), T_m, are equivalent. However, the freezing (or crystallisation) point is highly influenced by kinetics and is not always equivalent to the melting point.

Two types of crystallisation exist. Typically, during cooling, a system will crystallise from an amorphous liquid to a more organised solid structure. Crystallisation can also occur during heating, where an amorphous solid transitions to a crystalline solid, and is referred to as cold-crystallisation.

Crystallisation is a two-step process where nucleation centres must occur before crystal growth can begin. If the system has a high purity, it is more difficult for nucleation to occur as less defects and impurities are present to act as nucleation centres. The system is kinetically stable in the absence of nucleation centres and can be cooled far below its melting temperature, remaining in a supercooled liquid-like state.

The crystallisation temperature also depends on the rate of cooling. If a liquid is cooled quickly, the system has less time to organise itself into a highly ordered structure and less perfect crystals are formed. Lower crystallisation temperatures are observed when forming less perfect crystals. Conversely, a slow cooling rate allows this rearrangement to occur over a longer timescale forming more perfect thermodynamic crystals with a higher crystallisation point.

Thermal history

Figure S3 shows heating scans from -90 ^{o}C to different $T_{\max}$ values for samples of wet 1:10 ChCl:EG ($x_{\mathrm{ChCl}} = 0.09$). In Figure S3(a), the first heating ramp to 0 ^{o}C shows no thermal events (blue). The sample is then cooled to -90 ^{o}C and the following heating ramp is shown in green. No thermal events are observed at $T < 0$ ^{o}C, however above 0 ^{o}C we observe the start of an endothermic transition due to water evaporation. We then prepare a new sample pan (*i.e.* not the sample used in (a)), and increase $T_{\max}$ to 150 ^{o}C. The first run in Figure S3(b) shows the broad endothermic peak due to water evaporation, with no thermal events before this point. On the following heating ramp, we observe a series of exothermic and endothermic transitions below 0 ^{o}C, that appear to overlap. When $T_{\max}$ is increased to 200 ^{o}C as in Figure S3(c), during the first heating ramp water evaporates and so does the EG at approximately 200 ^{o}C. In the following heating ramp we observe a series of small exothermic peaks followed by an endothermic peak below 0 ^{o}C,

and a single endotherm at approximately 77 ^{o}C. At $T_{max} = 250$ ^{o}C, the water and EG evaporate completely in the first ramp (Figure S3(d)), resulting in a subsequent ramp that has a single endotherm at 77 ^{o}C due to a choline chloride solid-solid transition.[2,3]

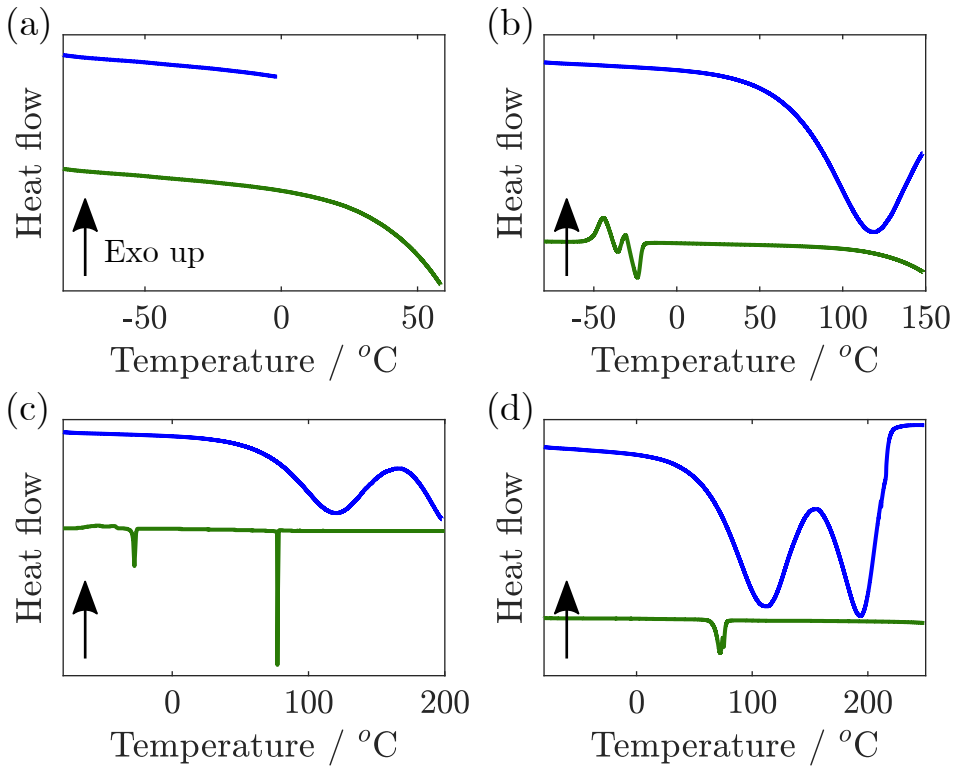

Figure S3 Heating DSC scans (offset vertically for clarity) highlighting the influence of thermal history on 1:10 ChCl:EG samples ($x_{ChCl} = 0.09$). The arrows indicate the direction of exothermic (exo) transitions. All heating ramps start at -90 ^{o}C. (a) First heating ramp at 10 ^{o}C/min to 0 ^{o}C (blue) and subsequent heating ramp at 10 ^{o}C/min to 60 ^{o}C (green). (b) First heating ramp at 10 ^{o}C/min to 150 ^{o}C (blue) and subsequent heating ramp at 10 ^{o}C/min to 150 ^{o}C (green). (c) First heating ramp at 10 ^{o}C/min to 200 ^{o}C (blue) and subsequent heating ramp at 1 ^{o}C/min to 200 ^{o}C (green). (d) First heating ramp at 10 ^{o}C/min to 250 ^{o}C (blue) and subsequent heating ramp at 10 ^{o}C/min to 250 ^{o}C (green).

These results highlight the importance of knowing the thermal history of the sample, as previous heating-cooling cycles can influence the observed thermograms quite dramatically. For example, if a liquid sample has been cooled below its freezing point quickly, a melting peak may not be observed in the subsequent heating cycle. Although thermodynamically the sample should crystallise below its melting point, quench cooling can kinetically inhibit crystallisation forming a more glassy liquid, and hence no subsequent melting transition.

A similar thermal history dependence was also observed when studying dry and ambient 1:2 ChCl:EG ($x_{ChCl} = 0.33$).

'Resetting' the Thermal History

With regards to the observations made above, we should highlight the preparation methods and consider the previous heating-cooling cycles. 'Resetting' the thermal history of the samples allows us to discuss the observed thermal events relative to the now known thermal history.

The thermograms in Figure 2 are from the heating ramp immediately after the heating-cooling cycle that defines the thermal history. The thermal history of each sample is as follows.

- Pure EG: heat from -70 ^{o}C to 50 ^{o}C at 10 ^{o}C/min, hold at 50 ^{o}C for 5 minutes, cool from 50 ^{o}C to -70 ^{o}C at 10 ^{o}C/min, hold at -70 ^{o}C for 5 minutes.
- Pure ChCl: heat from 0 ^{o}C to 200 ^{o}C at 10 ^{o}C/min, hold at 200 ^{o}C for 5 minutes, cool from 200 ^{o}C to 0 ^{o}C at 10 ^{o}C/min, hold at 0 ^{o}C for 5 minutes.
- $x_{\mathrm{ChCl}} = 0.01$: heat from -90 ^{o}C to 100 ^{o}C at 10 ^{o}C/min, hold at 100 ^{o}C for 5 minutes, cool from 100 ^{o}C to -90 ^{o}C at 10 ^{o}C/min, hold at -90 ^{o}C for 5 minutes.
- $x_{\mathrm{ChCl}} = 0.001$: heat from -90 ^{o}C to 50 ^{o}C at 1 ^{o}C/min, hold at 50 ^{o}C for 5 minutes, cool from 50 ^{o}C to -90 ^{o}C at 1 ^{o}C/min, hold at -90 ^{o}C for 5 minutes.
- All other x_{ChCl}: heat from -90 ^{o}C to 200 ^{o}C at 10 ^{o}C/min, hold at 200 ^{o}C for 5 minutes, cool from 200 ^{o}C to -90 ^{o}C at 10 ^{o}C/min, hold at -90 ^{o}C for 5 minutes.

Although faster heating rates increase the magnitudes (sensitivity) of the observed thermal events, the resolution is compromised. To construct a phase diagram, it is important that the resolution is maximised to obtain more accurate peak and onset temperatures, hence a slower heating rate should be used. However, a disadvantage of a slower heating rate is the increase in experiment time *e.g.* heating from 0 ^{o}C to 100 ^{o}C at 2 ^{o}C/min and 0.5 ^{o}C/min takes 50 minutes and 200 minutes (3.3 hours), respectively. The thermograms in Figure 2 were all heated at 1 ^{o}C/min to obtain reproducible peak and onset temperatures over reasonable experiment times.

Tammann Plot of Choline Chloride:Ethylene Glycol

Rather than relying on the mole fractions where the liquidus line is absent to define the eutectic composition, Rycerz [4] highlights the importance of producing Tammann diagrams when determining the eutectic compositions. [4,5] For a supposed eutectic event (the 'invariant'), the molar enthalpy of the transition can be plotted as a function of mole fraction. The integrated eutectic signal is expected to be largest at the eutectic point and, as a consequence of the lever rule, will decrease linearly either side of the eutectic point. [4]

Figure S4 shows the Tammann plot for the invariant transition at -28 ^{o}C observed in ChCl:EG mixtures. Surprisingly, the point at which the linear dependencies intersect (black-green and black-blue lines intersect at $x_{\mathrm{ChCl}} = 0.4$ and 0.5, respectively) does not coincide with our predicted window of $0.01 < x_{\mathrm{ChCl}} < 0.02$, nor does it coincide with previous studies. [6–10] Unfortunately, Tammann plots are complicated by the presence of other transitions and overlapping events. In the work of Rycerz, [4] a eutectic-like Tammann plot is shown to correspond to the incongruent melting of $RbTb_2Br_7$. It could therefore be possible that the Tamman plot shown in Figure S4 corresponds to an incongruent melting event.

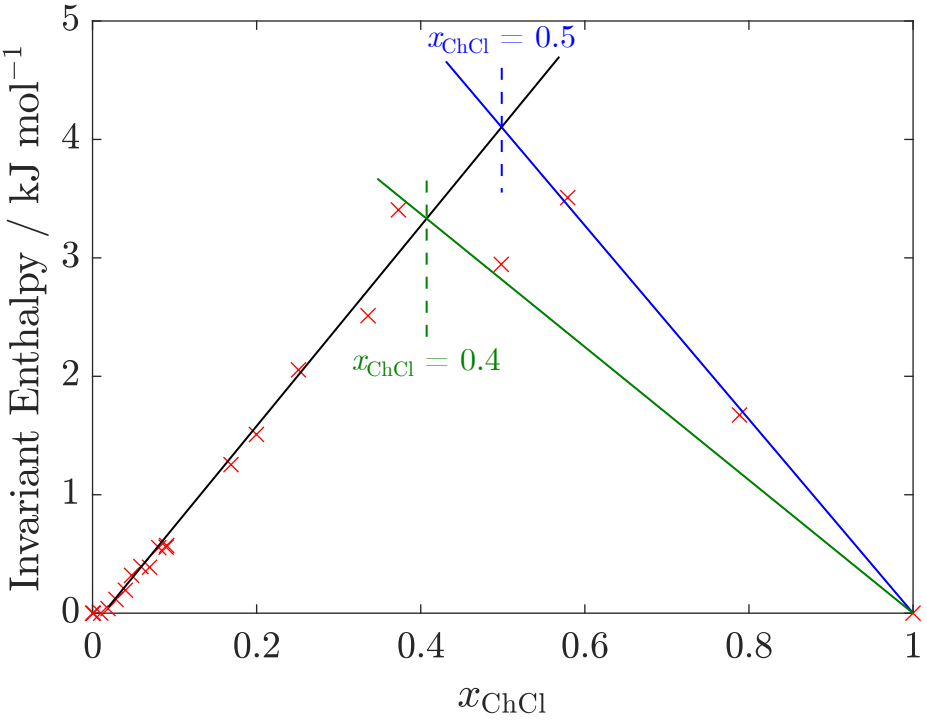

Figure S4 Invariant enthalpy as a function of ChCl mole fraction (Tammann plot) for the eutectic transition (the 'invariant') at -28 °C in observed in ChCl:EG mixtures (red crosses). The black line shows the linear dependence of invariant enthalpy with x_{ChCl} between $0.02 \leq x_{\mathrm{ChCl}} \leq 0.37$. Green and blue lines highlight two potential linear dependencies when $x_{\mathrm{ChCl}} \geq 0.37$. The green and blue lines intersect the black line at $x_{\mathrm{ChCl}} = 0.4$ and 0.5, respectively.

References

1. P. Gill, T. T. Moghadam and B. Ranjbar, *J. Biomol. Tech.*, 2010, **21**, 167.
2. I. M. Aroso, A. Paiva, R. L. Reis and A. R. C. Duarte, *J. Mol. Liq.*, 2017, **241**, 654–661.
3. R. L. Collin, *J. Am. Chem. Soc.*, 1957, **79**, 6086–6086.
4. L. Rycerz, *Journal of Thermal Analysis and Calorimetry*, 2013, **113**, 231–238.
5. A. Dańczak and L. Rycerz, *Journal of Thermal Analysis and Calorimetry*, 2016, **126**, 299–305.
6. R. K. Ibrahim, M. Hayyan, M. A. AlSaadi, S. Ibrahim, A. Hayyan and M. A. Hashim, *J. Mol. Liq.*, 2019, **276**, 794–800.
7. E. A. Crespo, L. P. Silva, J. O. Lloret, P. J. Carvalho, L. F. Vega, F. Llovell and J. A. Coutinho, *Phys. Chem. Chem. Phys.*, 2019, **21**, 15046–15061.
8. V. Agieienko and R. Buchner, *Phys. Chem. Chem. Phys.*, 2022, **24**, 5265–5268.
9. K. Shahbaz, F. S. Mjalli, M. Hashim and I. M. ALNashef, *J. Appl. Sci.*, 2010, **10**, 3349–3354.
10. A. Jani, T. Sohier and D. Morineau, *J. Mol. Liq.*, 2020, **304**, 112701.